Numerical Analysis of the Mechanical Behavior under Seismic Loading of Discrete Element Structures: Application to 3D Fractured Rock Masses, and Large Stone Course Buildings

Marc Vinches, Ali Rafiee, Claude Bohatier

NUMERICAL ANALYSIS OF THE MECHANICAL BEHAVIOR UNDER SEISMIC LOADING OF DISCRETE ELEMENT STRUCTURES: APPLICATION TO 3D FRACTURED ROCK MASSES, AND LARGE STONE COURSE BUILDINGS

Marc A. Vinches [1], Ali Rafiee [2], Claude E. Bohatier [3]

[1] CMGD, Ecole des Mines d'Alès,
6, Avenue de Clavières 30319 ALES CEDEX, France
e-mail : marc.vinches@ema.fr

[2] University of Zanjan, University Boulevard
P.O. Box 313, 45371-38111 ZANJAN, Iran
e-mail : ali_rafiee@znu.ac.ir

[3] LMGC-UMR5508, Université Montpellier II, CC048,
Place Eugène Bataillon 34095 MONTPELLIER CEDEX 5, France
e-mail: bohatier@lmgc.univ-montp2.fr

Keywords: Discrete elements, NSCD method, tridimensional geometry, masonry structures, fractured rock mass, recorded accelerogram.

Abstract: *Discrete element models have been extensively used, in 2D, in rock mechanics since the 1970's. For modeling masonry buildings in 3D, their application is more recent. This is mainly because of the often complex 3D geometry of the individual blocks composing the masonry: a complexity which has to be taken into account. The same complexity in 3D can be considered in rock mechanics problems.*

We propose to illustrate the influence of an accurate, and hopefully representative, 3D geometry of individual blocks, on the global behavior under a seismic loading of several structures. We will first present the cases of stone arches, as an academic example. We will then detail the behavior of two Roman masonry arched structures: the Julian Bridge and the Arles aqueduct. A last case study of masonry will present the analysis of the behavior of a classical brick house with a particular emphasis on the influence of the bricks and beams disposition, the presence of openings, the care given to the interlocking of the brick pattern on the angles of the building. Finally the analysis of the stability of a rock mass slope is presented, showing the capabilities of the NSCD method to cope with thousands of simultaneous contacts, under dynamic loadings.

1 INTRODUCTION

The analysis of the mechanical behavior of fractured rock masses lead to the development of the distinct element methods, at the beginning of the 1970's. The works of P. CUNDAL [1] are often considered at the origin of the development of these methods. The calculation of the reactions between the different elements assumed a small, but not zero, overlapping of the elements at the contact zone.

As presented by J.J. MOREAU [2], with the help of convex analysis and complementarity theory, other methods were developed based on the strict handling of the unilaterality and nonsmoothness. The Non-Smooth Contact Dynamics (NSCD) method, based on MOREAU's initial work, mainly dealing with the equation of dynamics, the Signorini relation as a non-smooth modeling of unilateral contact, and the frictional Coulomb's law, treated with fully implicit algorithms, can also deal with other interface problems, including cohesion, M. JEAN [3], M. JEAN et al. [4]. The computer code LMGC90® is based on the NSCD method, and all the examples presented in this paper, used this code, F. DUBOIS and M. JEAN [5]

Rather than describing again the main features of the NSCD method, available in the already given references, we present in the following sections, first an academic example of a tridimensional stone arch, on which different dynamic loads are applied, with a sensitivity analysis on the boundary conditions of the model; then two Roman bridge structures with the complexity of their block geometry and relative arrangement; and, last, a more modern house structure with thousands of bricks, and few metal beams, representative of a classical building technique from the beginning of the XXth century, in industrialized countries.

The application of the NSCD method to the analysis of the stability of a rock slope will be presented, involving several thousand blocks. The need for a realistic tridimensional model, and the comparison with results from a two dimension section, will be emphasized.

2 ANALYSIS OF A 3D STONE ARCH BEHAVIOR

2.1 Geometry description

The geometrical characteristics of the arch are shown in Fig. 1. The model consists of an arch composed of 11 blocks with a supporting base that will be subjected to a vibration in three directions. The numbers beside the blocks in this figure represent the order of the blocks in the model. They will be referred to in the post-processing section. The blocks in the model are 25 cm thick and 25 cm wide.

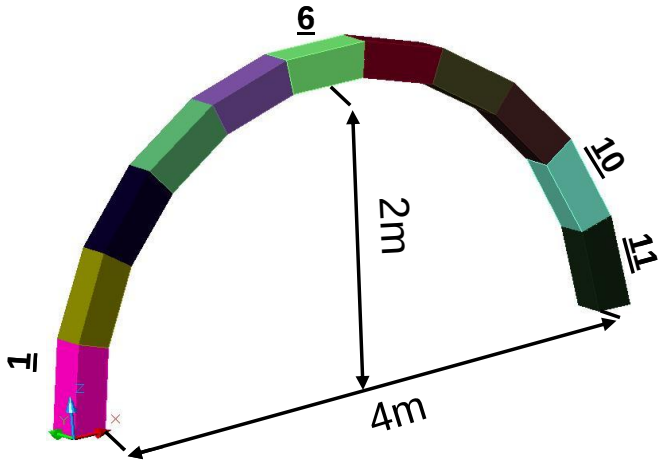

Figure 1 : Geometry of the arch with eleven blocks

2.2 Mechanical assumptions and parameters, loads, and boundary conditions

This simple arch structure is studied for different mechanical conditions affecting the behaviour of the interface between the blocks and also between the blocks and the supporting element. Therefore, several simulations are performed with the same geometrical configuration, first, with changes of interaction laws, and, then, for a given law, with different values of their parameters.

In all the following calculations, the blocks are assumed to be rigid, and their density is 2000 kg/m^3. Table 1 presents different sets of laws and parameters used in four different models. More cases were studied and are presented in more detail in A. RAFIEE et al.[6]

Table 1: Interaction contact parameters used in the four models, (a) model 1: embedded, (b) cohesive models 2 and 3: with the same cohesive condition between ground and blocks, and the 11 blocks, (c) model 4: dry friction.

(a)

Embedded model		Static friction coefficient	Dynamic friction coefficient	Normal cohesion (Pa)	Tangential cohesion (Pa)
1	Blocks	0.7	0.6	0.1×10^4	0.7×10^3
	G & B	0.7	0.6	0.1×10^6	0.7×10^5

(b)

Cohesive models (G & B, B 1-11)	Static friction coefficient	Dynamic friction coefficient	Normal cohesion (Pa)	Tangential cohesion (Pa)
2	0.7	0.6	0.1×10^6	0.7×10^5
3	0.7	0.6	0.1×10^4	0.7×10^3

(c)

Dry contact model	Friction coefficient (Blocks)	Friction coefficient (G & B)
4	0.7	0.9

(* G: Ground, B: Blocks)

The arch, resting on its base, was loaded with the input of a velocity on this base, obtained from the recorded accelerogram of the Zanjiran earthquake, Iran, June 20th 1994 [7]. The accelerogram in three directions is presented in Fig. 2.

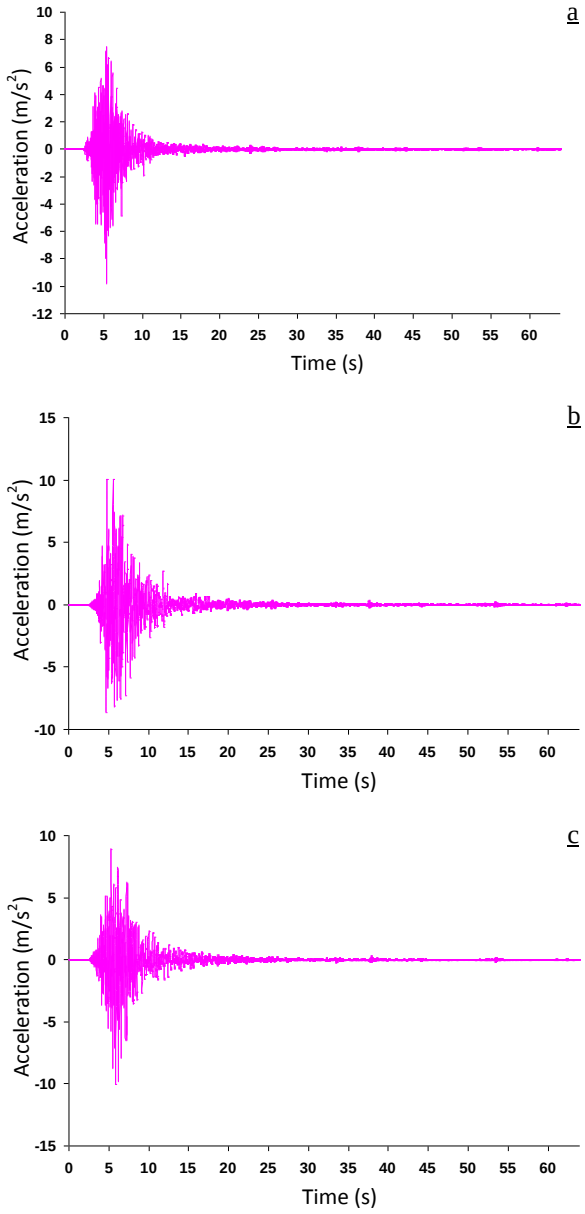

Figure 2 : Accelerogram in three orthogonal directions :
(a) vertical, (b) parallel to the arch, X direction, (c) perpendicular to the arch, Y direction

2.3 Results and analysis

Fig. 3 shows the results obtained on the four models after several seconds of seismic loading. One can notice that models 1 and 2 remain stable. The model 3 collapses probably because of a much weaker cohesion (one hundredth of that of model 2), with no apparent rotation of the blocks, out of the arch plane. The model 4 with no cohesion at all seams to resist less than model 3.

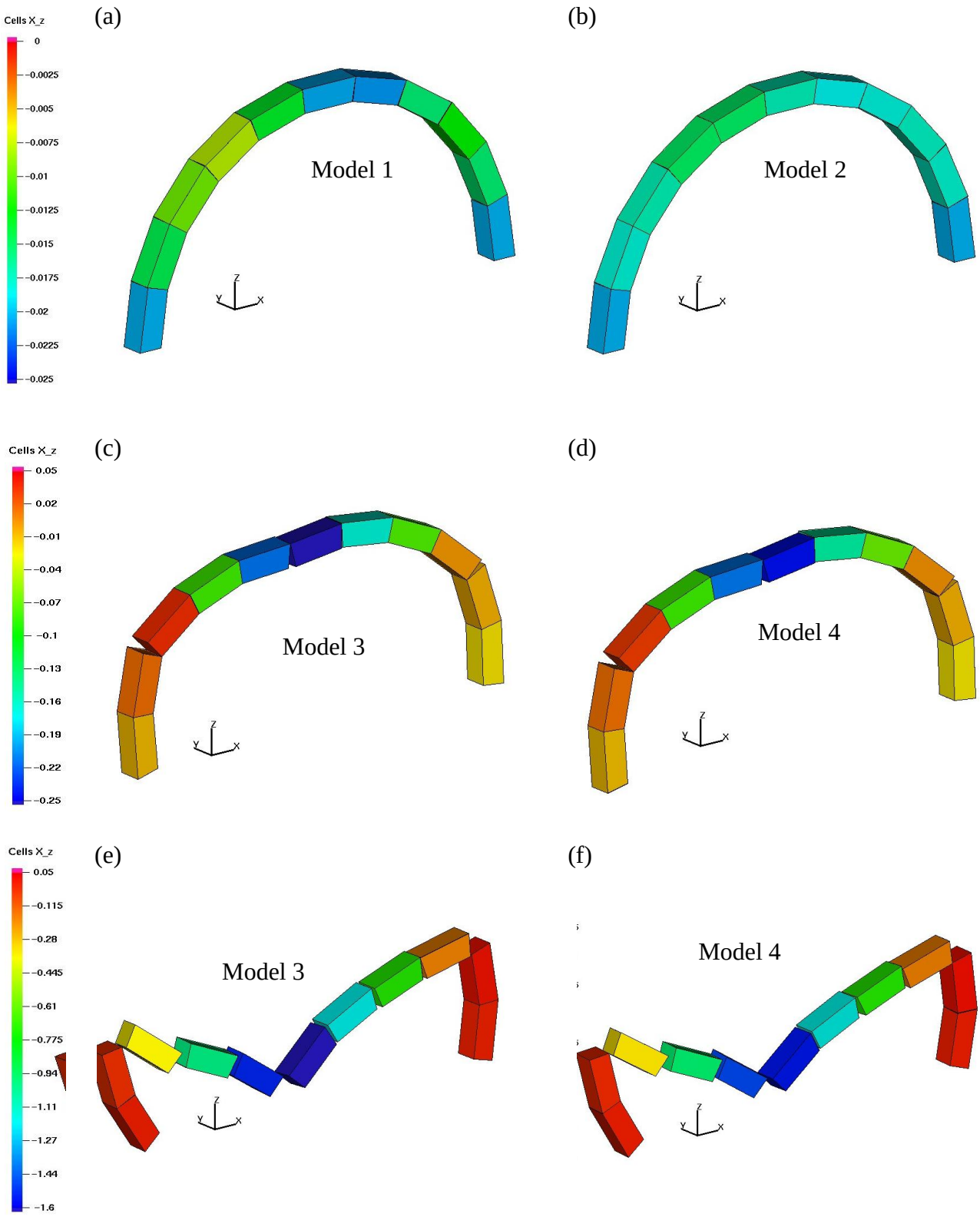

Figure 3 : Collapse mechanism of the four models, ((a) and (b)) model 1 and 2 after 7 seconds of seismic loading, ((c) and (d)) model 3 and 4 after five seconds, and ((e) and (f)) model 3 and 4 after 5.4 seconds.

3 ROMAN STONE BRIDGE MODELS

3.1 The Julian Bridge, on the Via Domitia, France.

The Julian bridge, on the Roman Via Domitia, the main road linking Italy to Spain at that time, was build during the first century B.C.. It is composed of three arches, the largest having a span of 16 meters, the smallest 10,2 m, Fig. 4. The maximum height over the water is close to 10 m. Its total length is 117,70 m, with a width of 5,90 m. More details can be found in [8]

Based on in situ measurements, a 2D model of 1118 meshed distinct elements blocks was created, with a Young modulus of E=16 GPa, a Poisson ratio of 0,25, a density of 1820 kg/m^3, and a friction coefficient of 0,8. A linear elastic isotropic behavior of the material was assumed. A comparison with the results obtained with a rigid blocks model was made. We summarize in this paragraph the main results, presented in a more detailed form in [9].

Figure 4 : The Julian bridge, on the Via Domitia. One can notice the holes made between the stone blocks, on the outside of the arches, to steal the iron staples used to bind the stones together.

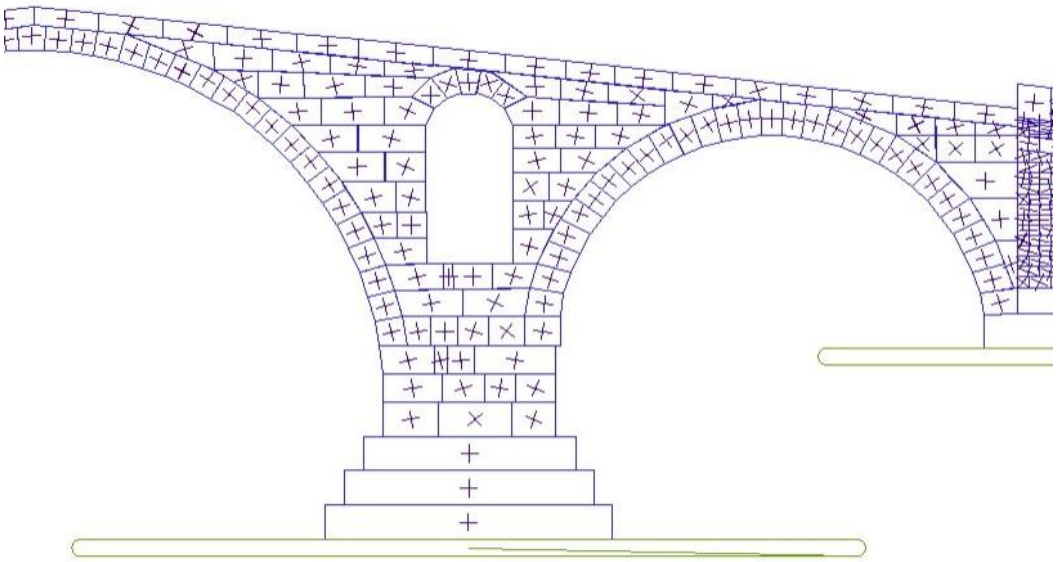

Figure 5 : The Julian bridge. Detail of the principal stress directions in the elastic model.

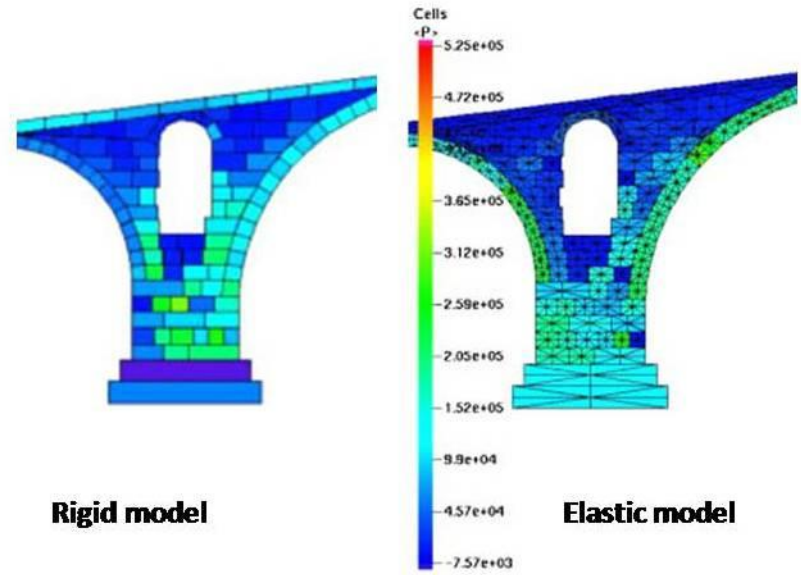

Figure 6 : The Julian bridge. Details of the spherical stress tensor invariant.

On Fig. 5, one can see the influence of the block geometry on the local orientation of the principal stress. On Fig. 6, we can notice that the spherical stress tensor invariant might change locally between the rigid and the elastic models.

Due to the obviously 3D interlocking nature of the stone arrangement in the real structure, visible on Fig. 7, and not taken into account in the previous model, a tri-dimensional model was set up [10]. We checked that the stability of the structure was achieved with virtually no displacements of any blocks, Fig. 8. Among other tests, this allowed us to check the contact detection algorithm good performance, in 3D, Fig. 9.

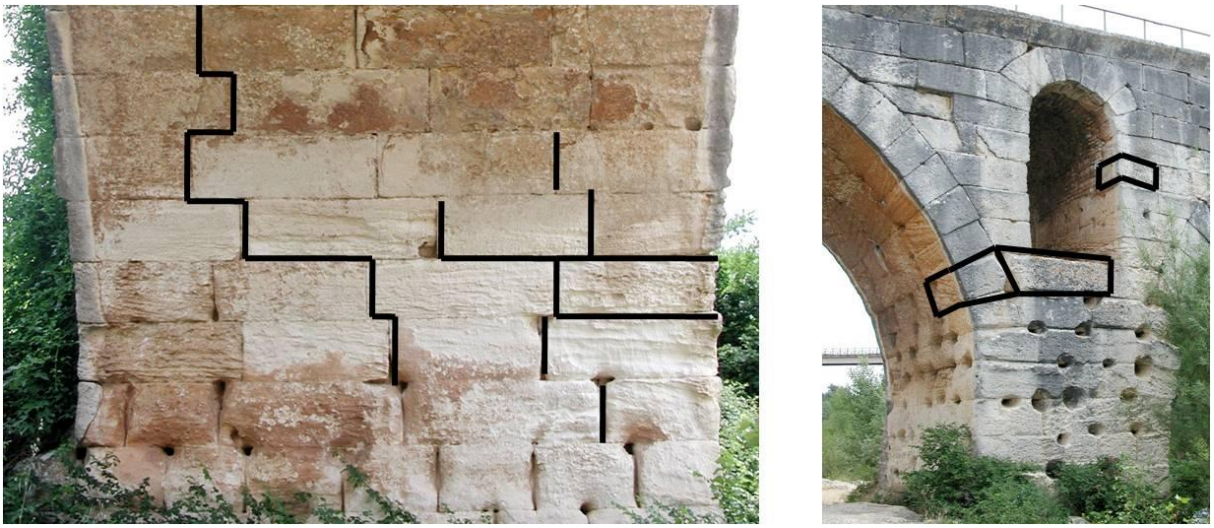

Figure 7 : The Julian bridge. Details of the tri-dimensional stone-by-stone arrangement.

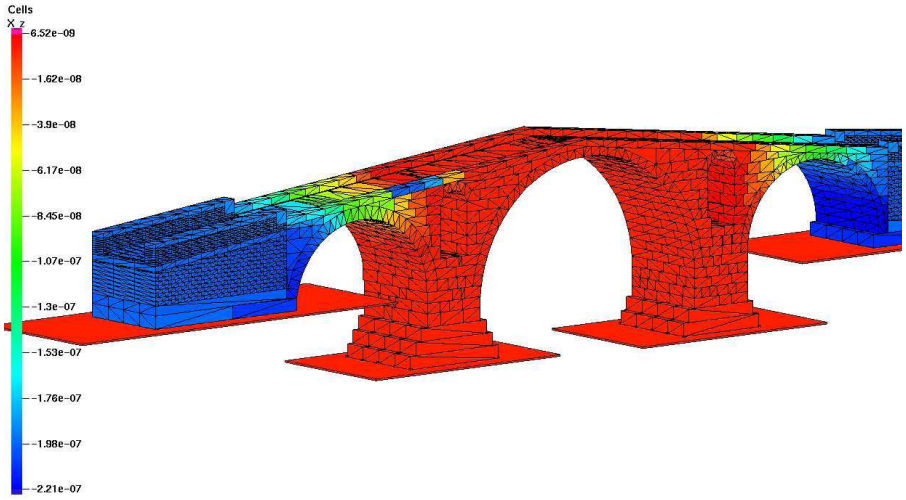

Figure 8: The Julian bridge: Accurate geometrical description of the blocks: Numerical displacements of a few microns for the different blocks, under gravity.

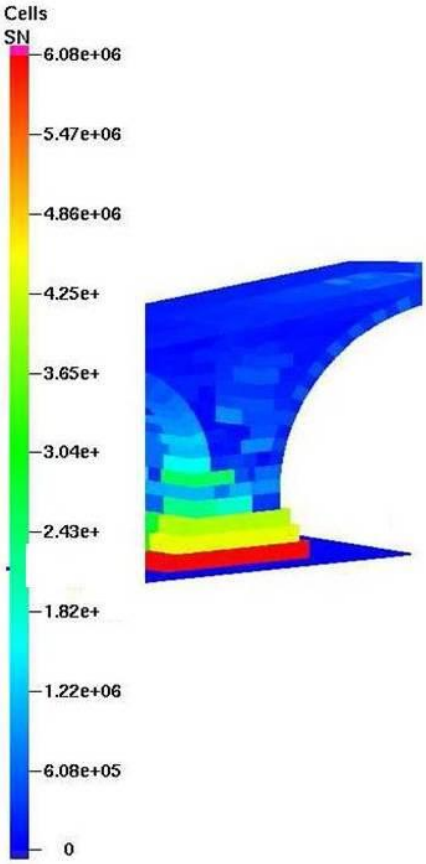

Figure 9 : The Julian Bridge: Detail of the vertical load on each block, on one pile [10].

3.2 The Arles and Barbegal aqueducts, at the Vallon des Arcs, Fontvielle, France.

The Vallon des Arcs aqueducts are one of the best preserved Roman antique remains of the Arles aqueduct sections. These aqueducts were mainly investigated, in the end of the XXth century by Philippe Leveau [11]

In order to test the capacity of our software, concerning the geometry transfer of thousands of blocks, the new algorithm for the detection of contacts in the case of collisions between blocks, and the possibility to reproduce the effects of a real earthquake on such a structure, by the introduction of a recorded accelerogram, we modeled a section of the first Arles aqueduct, based on the hypothesis of Leveau, and observed preliminary results given by the model, with the aim of exploring similarities and differences with the observed remains of the aqueduct. A detailed description of the model, and of the tests carried out on it, is available in [12]

The following figures give an illustration of the modeled structures, of the computer model geometry, Fig. 10, and of some results, considering the blocks of the large stone course first Arles aqueduct as rigid elements, Fig. 11.

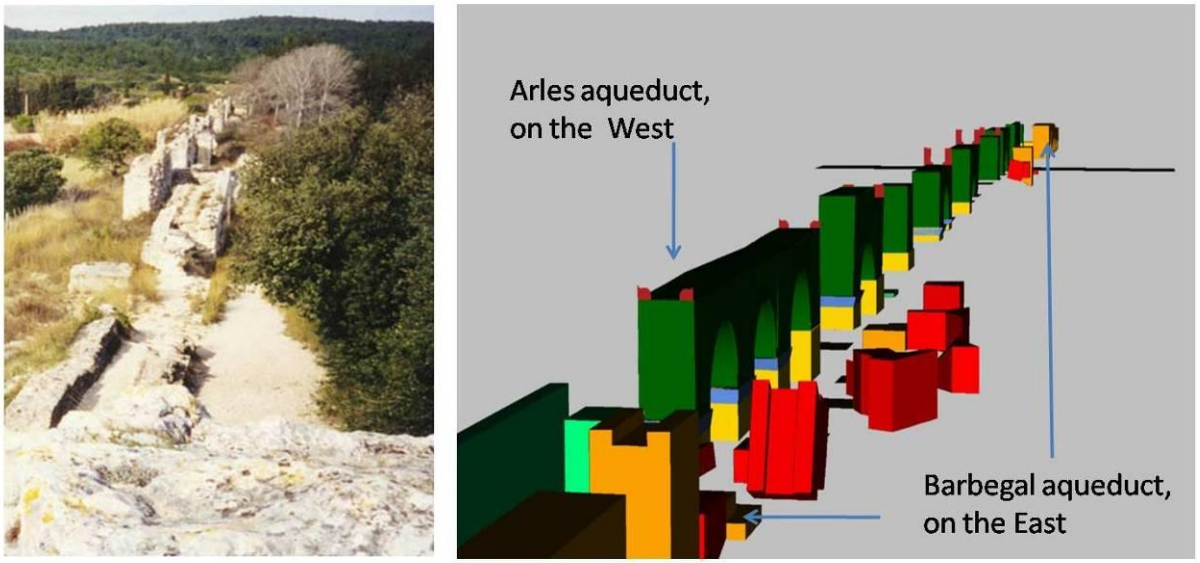

Figure 10: Arles and Barbegal aqueducts : general view of the site.

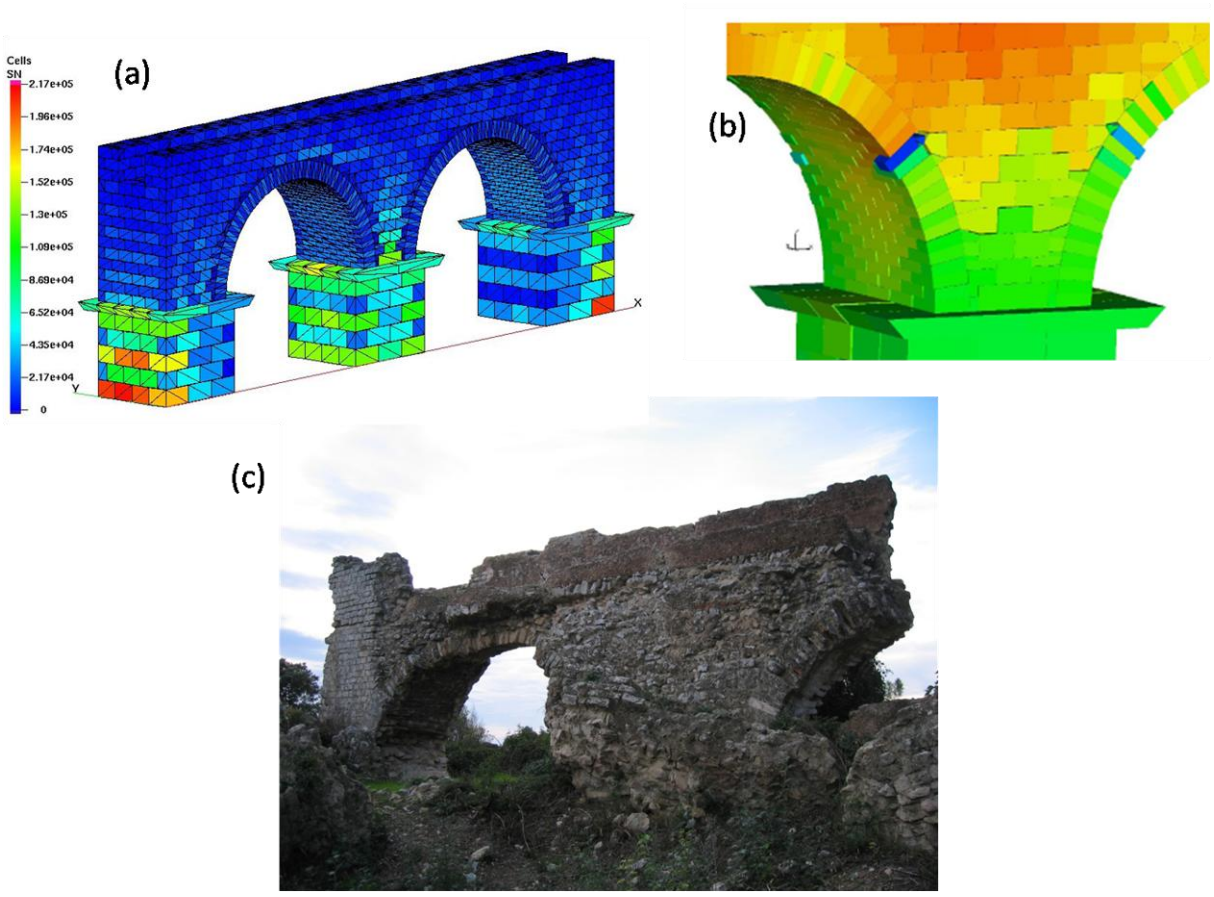

Figure 11 : Arles and Barbegal aqueducts : Rigid model, (a) original geometry, with load distribution before the earthquake, (b) final geometry with the vertical displacement after 4 seconds of the Zanjiran recorded earthquake simulation (see Fig. 2), (c) a section of the real aqueduct today

4 BRICK AND BEAM STRUCTURE

4.1 Geometry description.

Fig. 12 presents the geometry of a beam and brick structure, representing a classical technique used in the industrialized countries at the beginning of the XXth century. One should notice that the structure presents different peculiarities: concerning the side walls, only one has an aperture; concerning the building angles, only one side presents an interlocking of the bricks; concerning the main openings, a discharge arch and a massive lintel have been inserted, but no reinforcement is present in the form of interlocking of bricks around the opening. Fig. 12(a)shows the front of the house, Fig.12 (b) the back of the house, with a door. One can notice, on this figure, the well balanced distribution of vertical loads on the bricks. The color intensity is correlated to this vertical load.

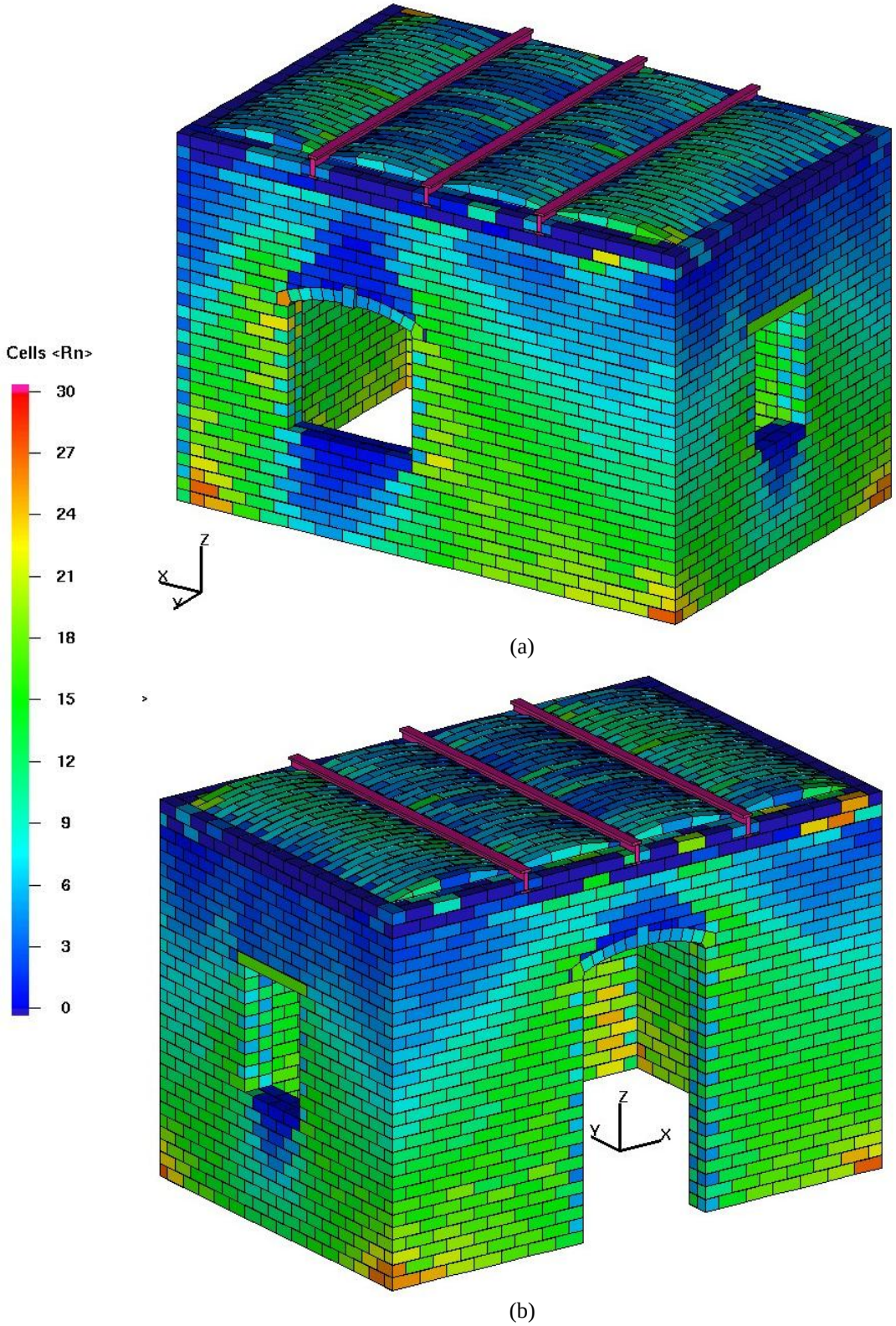

Figure 12: Two views of the geometry of the traditional beam and brick home, ((a) and (b)) relative load distribution over the structure blocks.

4.2 Mechanical assumptions and parameters, loads, and boundary condition description.

The beams and the bricks of the model are supposed to be rigid. The parameters presented in table 1 for the second model are used for this structure: the same cohesive condition is considered for the contact surfaces between the blocks as well as the contacts between the blocks and the ground. The structure is subjected to the recorded seism excitation illustrated in Fig. 2 during the first 20 seconds. The density of the bricks is 2,5 kg/m^3, and the density of the steel used in the beams is assumed to be 7850 kg/m^3.

4.3 Results and analysis.

The following figures show the vertical displacement of the different components of the structure during the solicitation.

During the first four seconds of this seismic excitation, as can be seen in Fig 13(a), the structure shows an acceptable resistance against the imposed vibration, and the negligible displacements can be distinguished.

After five seconds of the seismic vibration which is accompanied with intensive vibration (see Fig. 2), the structure begins to fail. The collapse of this masonry building is triggered by the two lateral arches of the roof. These two arches begin to fail (Fig. 13(b)), and consequently the lateral walls are pushed outward.

It should be noted that the construction techniques applied of these two side walls are deliberately chosen different. In the right side wall, the bricks in the corners are crossed with the bricks of the other two walls, whereas in the left side wall the bricks are crossed with only the bricks of the back wall. Consequently the left wall shows a weaker resistance during the seismic excitation. As can be seen in Fig. 13(b) the left wall begins to collapse.

This failure is more evident in Fig.13(c), where the left wall separates from the rest of the structure. In this step (after 5.5 seconds), all of the roof arches have collapsed and only the right remains approximately intact.

At the sixth second (Fig. 13(d)) the arches over the door and the windows begin to collapse.

During the last steps (8th and 9th seconds, respectively Fig. 13(e) and (f)), the front and back walls also start to fail.

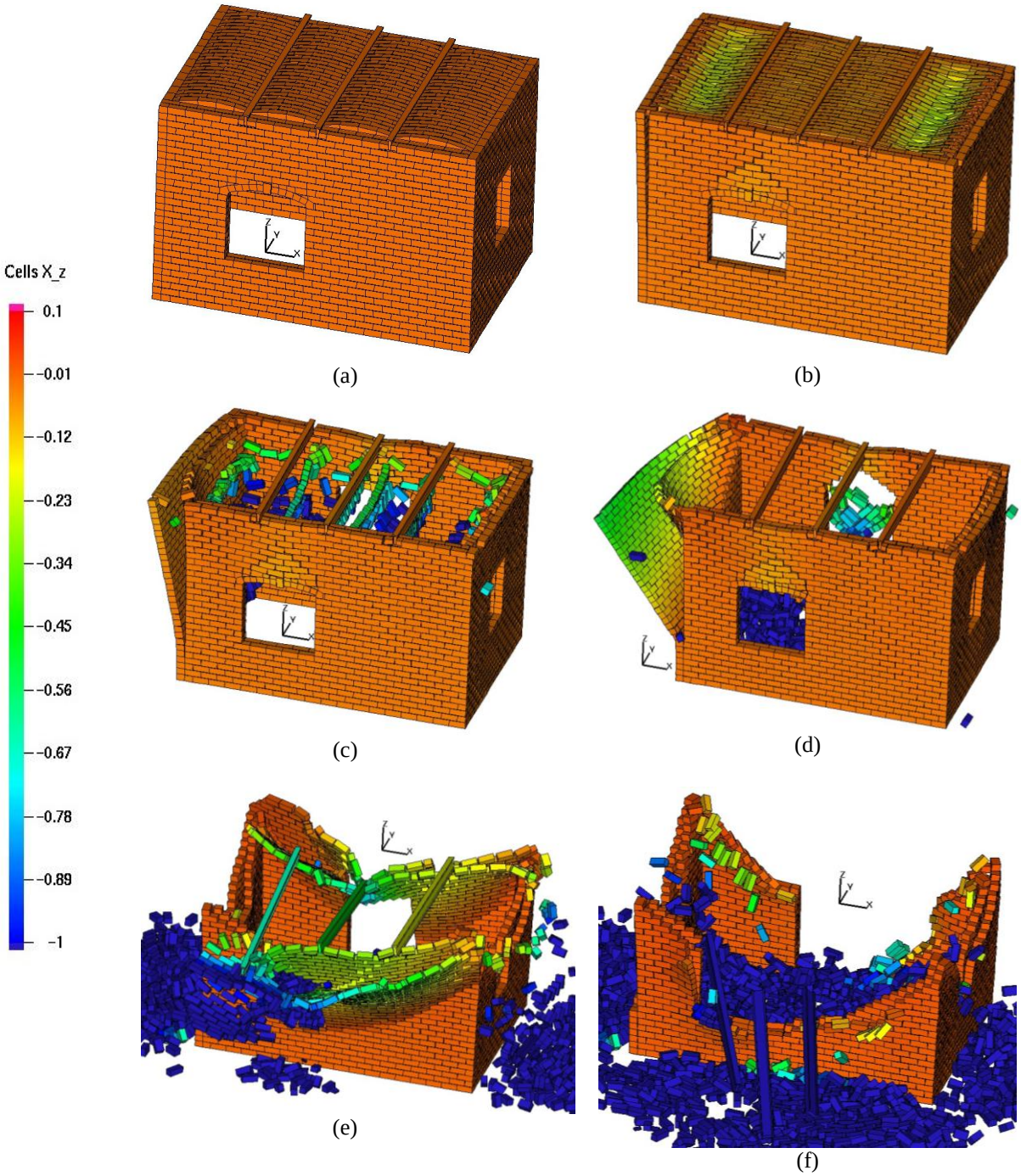

Figure 13 : Successive steps of the structure collapse caused by the real earthquake presented in Figure 2, after (a) 4 seconds, (b) 5 seconds, (c) 5.5 seconds, (d) 6 seconds, (e) 8 seconds, and (f) 9 seconds.

5 ANALYSIS OF A ROCK SLOPE

5.1 Geometry description

The Pallat ravine is located in the South of France, in the Pyrenees Mountains, Fig. 1. Due to an increasing traffic in winter, it was decided to widen the road in the fractured rock mass slope, above the railway. A detailed presentation of the site, and of the techniques developed to get a realistic model of the fracture network geometry is available in [13]

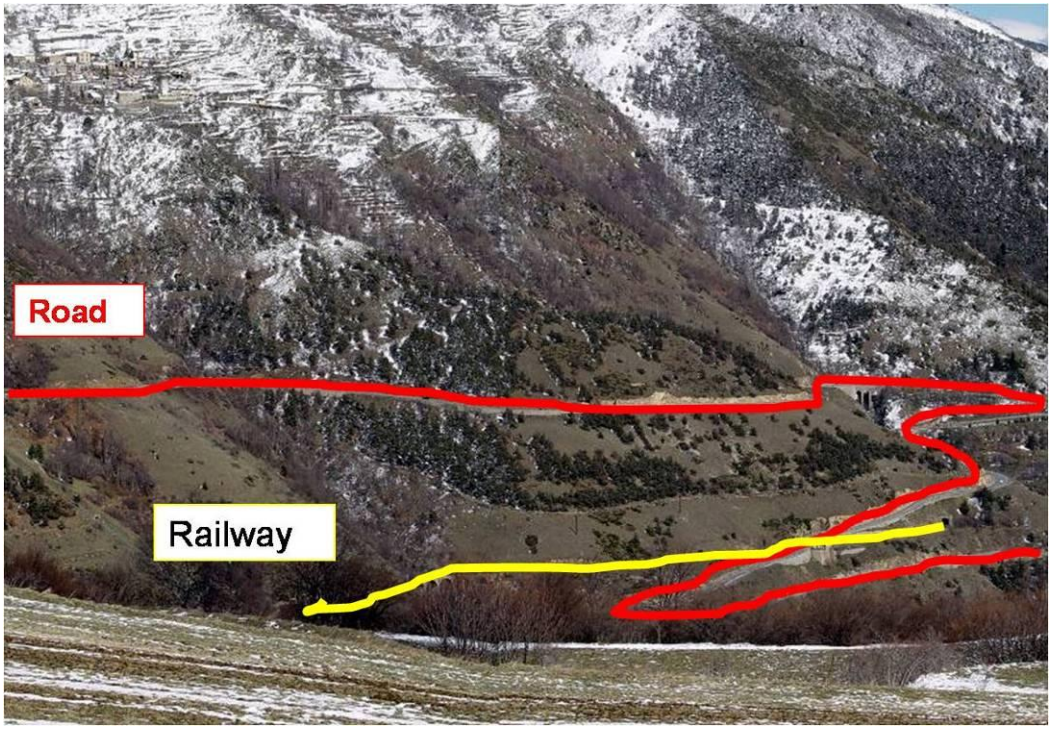

Figure 14 : General view of the Pallat ravine

5.2 Mechanical assumptions and parameters, loads, and boundary conditions

From a tridimensional fracture network model, a section is obtained, and studied using the LMGC90 software. The blocks are supposed to be rigid, and the contact law is a Coulomb friction law, with a friction coefficient of 0,7. The density of the stone is 2000 kg/m^3. The blocks cannot penetrate the horizontal base, nor pass the vertical line on the left of the 2D model, Fig. 15(a); they cannot intersect the horizontal base, neither the lateral vertical faces, nor the vertical face at the back of the 3D model. The gravity applies vertically (9,81 m.s^{-2}).

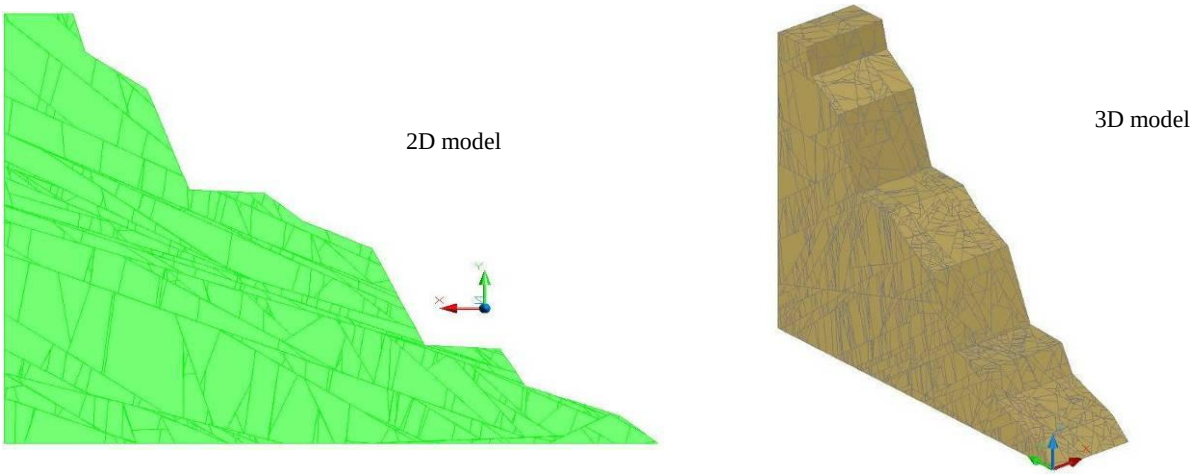

Figure 15 : Geometry of the slope model, (a) in two dimensions, (b) in three dimensions

5.3 Results and analysis.

Fig. 16 shows the horizontal displacement of the different blocks on the slope. If some conclusions had to be drawn from Fig. 16 (a), they might have been very different from those based on the analysis of block instability on Fif.16 (b). This result is very well known in the rock mechanics community, this case in just another illustration of the importance of a realistic 3D model.

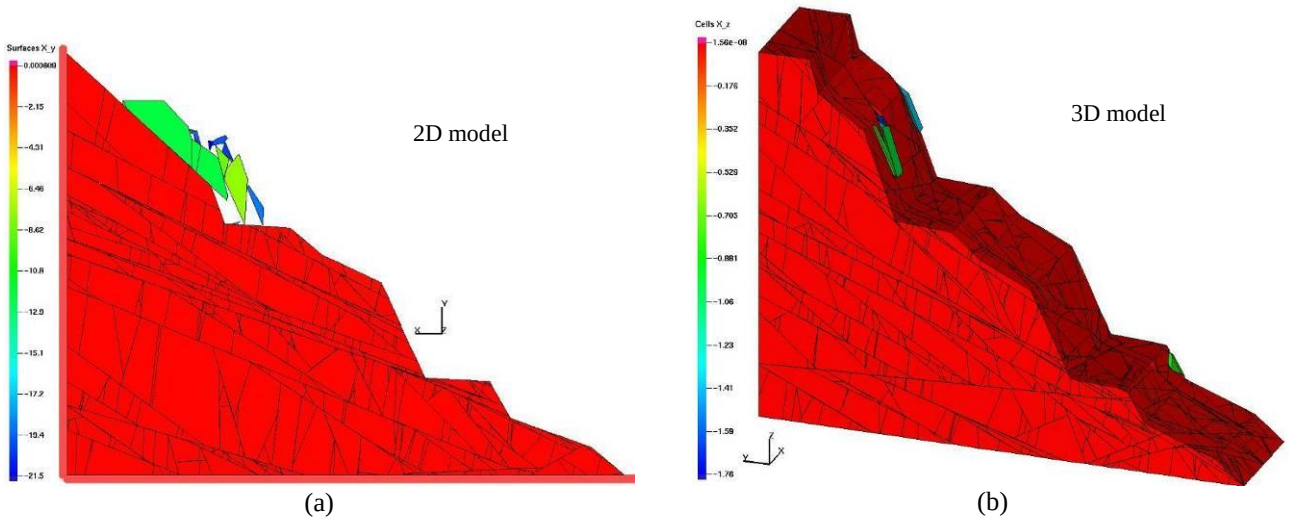

Figure 16 : Geometry of the slope model, (a) in two dimensions, (b) in three dimensions

More detailed analyses, including rock slope behaviour with seismic loadings are presented in Ali Rafiee [14].

6 CONCLUSIONS

We have presented on an academic example that the NSCD method, implemented in the LMGC90 code, allows to deal with different types of non smooth friction law, with and without cohesion, taking into account recorded accelerograms.

Concerning the behavior of real masonry structures, the Roman bridge, and the Roman aqueducts examples illustrate the need to have tridimensional models in order to analyze the influence of the block arrangements on the forces distribution in real structures.

The last example of an ordinary masonry building, composed of bricks and beams, allows us to analyze the importance of technical rules of art, such as a special treatment of the structure angles, lintels, or beam disposition.

More complete models can be tested including reinforcement using post-stressing cables, and a combination of realistic mechanical behavior of the block interface, accurate tridimensional description of thousands of blocks, and the loading of the structure using recorded or user specified accelerograms [14].

AKNOWLEDGEMENTS

The authors wish to thank Dr. Brahim Chétouane, from the Military Academy of Tunisia, Dr. Robert Pérales, and Dr. Frédéric Dubois from the University of Montpellier, France, for their contribution to different aspects of the works on masonry structures presented in this paper.

REFERENCES

[1] Cundall P.A., A computer model for simulating progressive large scale movements of blocky rock systems. *Proceedings of the Symposium of the International Society of Rock Mechanics, Nancy, France*, vol. 1, pp.132-150, 1971

[2] Moreau J.J., Some basics of unilateral dynamics, *In: IUTAM Symposium on Unilateral Multibody Contacts, F. Pfeiffer and Ch. Glocker (eds.), Kluwer Academic Publisher*, pp. 1-14, 1999.

[3] Jean M. 1999. The non-smooth contact dynamics method. *Computer Methods in Applied Mechanics and Engineering*, 177, pp. 235-257.

[4] Jean M., Acary V., Monerie Y., Non Smooth contact dynamics approach of cohesive materials. *Philosophical Transactions: Mathematical, Physical & Engineering, The Royal Society, London A*, A359 (1789), pp 2497-2518, 2001.

[5] Dubois F, Jean M, LMGC90 une plateforme de développement dédiée à la modélisation des problèmes d'interaction, *Actes du sixième colloque national en calcul des structures, CSMA-AFM-LMS*, vol. 1, pp 111-118, 2003.

[6] A. Rafiee, M. Vinches, C. Bohatier, Application of the NSCD method to analyse the dynamic behaviour of stone arched structures. *International Journal of Solids and Structures*, **45**, issues 25-26, 6269-6283, 2008

[7] ISMN. Zanjiran earthquake, Iran, June 20th 1994, http://www.bhrc.ac.ir/ISMN/SHABAKEH/accelerograms/earthquake/ten_years/zanjiran/zanjiran.htm.

[8] G. Barruol, J.-M. Mignon, L'entretien et la mise en valeur des ponts antiques encore en usage: l'exemple du Pont Julien d'Apt, *to be published in the proceedings of Colloque « Les ponts Routiers en Gaule Romaine », 8-11 octobre, 2008.*

[9] B. Chetouane, F. Dubois, M. Vinches, C. Bohatier, NSCD discrete element method for modelling masonry structures, *International Journal for Numerical. Methods in Engineering, **64**, 65-94, 2005*

[10] R. Perales, Modélisation du comportement mécanique par elements discrets des ouvrages maçonnés tridimensionnels. Contribution à la définition d'éléments de contacts surfaciques. *Doctorate thesis, Laboratoire de Mécanique et de Génie Civil, Université Montpellier II,* 239 p., 2007.

[11] Ph. Leveau, Les Moulins de Barbegal, les ponts-aqueducs du Vallon des Arcs et l'histoire naturelle de la vallée des Baux (Bilan de six ans de fouilles programmées), *Comptes Rendus de l'Académie des Inscriptions et Belles-Lettres*, 115-144, 1995.

[12] A. Rafiee, M. Vinches, C. Bohatier, Modelling and analysis of the Nîmes arena and the Arles aqueduct subjected to a seismic loading, using the Non-Smooth Contact Dynamics method, *Journal of Engineering Structures,* **30**, 3457-3467, 2008.

[13] A. Rafiee, M. Vinches**,** Application of Geostatistical Characteristics of Rock Mass Fracture Systems in 3D Model Generation. *International Journal of Rock Mechanics and Mining Sciences*, **45**, 644-652, 2008.

[14] A. Rafiee, Contribution à l'étude de la stabilité des massifs rocheux fracturés : caractérisation de la fracturation in-situ, géostatistique et mécanique des milieux discrets. *Doctorate thesis, Laboratoire de Mécanique et de Génie Civil, Université Montpellier II,* 271 p., 2008.